Indian J Phys (December 2013) 87(12):1189–1197
DOI 10.1007/s12648-013-0363-8

ORIGINAL PAPER

Structural studies on picolinium maleate crystal by density functional methods

S Gunasekaran[1], K S Kannan[1], S Loganathan[2], G Anand[2] and S Kumaresan[3]*

[1]PG and Research Department of Physics, Pachaiyappas College, Chennai 600030, India

[2]Department of Sciences, Arulmigu Meenakshi Amman College of Engineering, Vadamavandal 604410, India

[3]PG and Research Department of Physics, Arignar Anna Government Arts College, Cheyyar 604 407, India

Received: 02 May 2013 / Accepted: 09 July 2013 / Published online: 25 July 2013

Abstract: The optimized geometry and vibrational frequencies of picolinium maleate (PM), an organic non-linear optical material, was obtained by ab initio DFT/B3LYP level with complete relaxation in the potential energy surface using 6-311G(d,p) basis sets. The Fourier-transform infrared (FT-IR) spectrum of PM was recorded in the region 4,000–400 cm^{-1}. The harmonic vibrational frequencies were calculated and scaled values had been compared with experimental FT-IR spectrum. The optical non-linearity arose from intermolecular hydrogen bonding between centro-symmetric picolinic acid and maleic acid. The DFT study was aimed at identifying intermolecular hydrogen bonding nature and comparing the calculated values with the XRD data. Analysis of experimental 13C shielding parameters was supported by DFT theoretical calculations carried out within the gauge-including atomic orbital and the spectra estimations were performed using ChemPro 8.0. It was found that chemical shifts obtained with ChemPro 8.0 were due to the substitution effects. The charge density distribution and site of chemical reactivity of molecules were obtained by mapping electron density isosurface with electrostatic potential surfaces. The scaled frequencies are comparable with the experimental frequencies. Energy span as calculated by ZINDO method, between the highest occupied molecular orbital and the lowest unoccupied molecular orbital of PM is −8.9697 and −1.5477 eV.

Keywords: Picolinium maleate; Non linear optics; HOMO–LUMO; Hydrogen bonding

PACS Nos.: 78.30.Jw; 78.40.Dw; 61.05.Qr

1. Introduction

Second-order nonlinear optical (NLO) materials are much attracted in recent research work because of their potential applications in the field of optoelectronics. In recent years, organic molecular NLO materials have been intensely investigated due to their high nonlinearities, rapid response to electro-optic effect as compared to inorganic NLO materials [1–5]. Organic crystals have been extensively studied due to their nonlinear optical (NLO) coefficient being often larger than those of inorganic. Combinations of amino acids with organic salts are promising materials for optical second harmonic generation. New nonlinear optical frequency conversion materials can have a significant impact on laser technology, optical communication and optical data storage technology [6]. The search for new frequency conversion materials over the past decade has concentrated primarily on organic compounds [7, 8] and many organic NLO materials with high nonlinear susceptibilities have been discovered. Amino acids are organic molecules that contain a carboxyl group (–COOH) as well as amino group (–NH2). In solid state, amino acids contain a protonated amino group (NH3+) and deprotonated carboxylic group as well as amino group (NH2). This dipolar nature exhibits peculiar physical and chemical properties in amino acids which makes them an ideal candidate for NLO application [9–12]. High performance of electro-optical switching for telecommunication and optical information processing are based on materials with high nonlinear optical properties. The search for new frequency conversion materials in recent years has concentrated on semi-organic

*Corresponding author, E-mail: yeskay72@yahoo.com

complexes [13]. Though inorganic materials or semiorganic materials have higher thermal stability than that of organic, their molecular hyperpolarizability plays vital role for second harmonics. In the present investigation picolinium and meleate are subjected to density functional study for their intermolecular and intramolecular hydrogen bonding and π–π* interactions. For the proper assignment of vibrational fundamentals and to understand effect of hydrogen bonding on the characteristic frequencies of the title compound normal coordinate analysis has been carried out.

2. Experimental details

The FTIR spectra of PM have been recorded in the region 4,000–400 cm^{-1} by using KBr windows with Bruker IFS 66 V spectrometer. A KBr beam splitter and liquid nitrogen cooled mercury-cadmium-tellurium (MCT) detector have been used to collect the mid infrared spectra. The UV–vis transmission spectrum of PM crystal is recorded in the range 190 and 1,100 nm using PerkinElmer Lamda 35 UV–VIS-NIR spectrometer, covering the entire visible and near infrared region. The spectral resolution for both FTIR and UV–vis is 2 cm^{-1}.

3. Theoretical calculations

The density functional theory (DFT) calculations were performed for the title compound, the initial geometry taken from crystallographic measurements was taken as the starting geometry for density functional theory (DFT) optimization. The geometry was optimized first, at semi-empirical level using Austin Model (AM1) method from the Chemsoft package and then at Hartree Fock (HF) and DFT level using the Becke 3 Lee–Yang–Parr (B3LYP) functional at 6-31G basis set with the help of GAUSSIAN-03 package [14]. Isotropic 1H- and 13C-nuclear magnetic shielding constants of this compound were calculated by employing the direct implementation of the gauge including-atomic-orbital (GIAO) method at the B3LYP density functional theory using 6-31G basis set. By combining the results, using graphical interface, GAUSSVIEW program with symmetry considerations, vibrational frequency assignments were made with a high degree of accuracy.

4. Results and discussion

4.1. Geometry analysis

The optimized structure parameters of PM by ab initio HF and DFT (B3LYP) levels with the 6-311G basis set in accordance with the atom numbering scheme given in Fig. 1. The molecules possessing C_1 point group symmetry with 72 fundamental modes of vibrations and are active in IR region. The X-ray experimental data on the geometrical parameters of PM are available in literature [15] and computed results are compared with the experimental data.

4.2. Conformational analysis

Molecular structure of PM is shown in Fig. 1. The bond length and bond angles of the structure of PM have been calculated by using B3LYP method at 6-311G(d,p) basis set. Picolinic acid forms well defined crystalline charge transfer (CT) with anion carboxylic acid through N···H···O and C···H···O hydrogen bonds. The present investigation aims to identify the direction of specific N···H···O bond between $–NH_2$ group and O^- group in the anion. The bond length between N–H···O is 1.638 Å and the observed value is at 2.28 Å. It is very close agreement with experimental

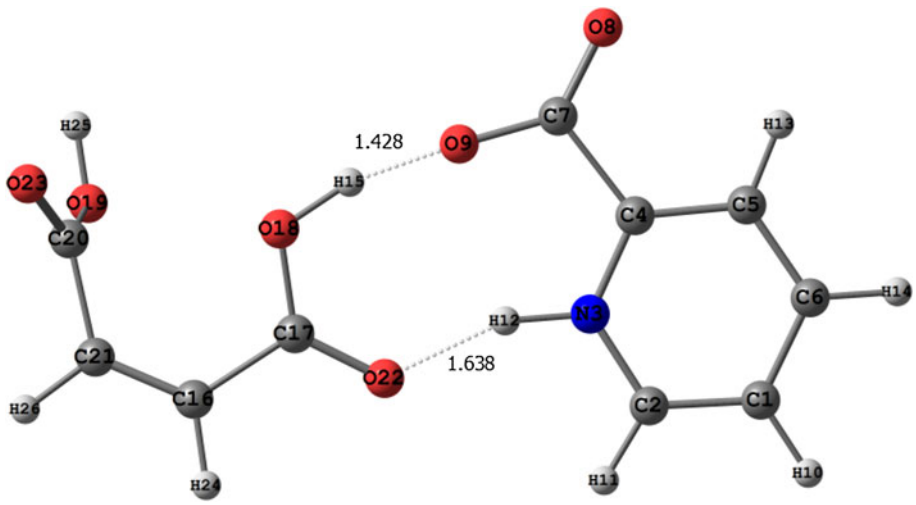

Fig. 1 Molecular structure (with atoms numbering) of PM at B3LYP/6-311G(d,p) basis set

data [16]. The average C–H bond length in the aromatic ring calculated by B3LYP/6-311G(d,p) is 1.067 Å. It is less than C–H bond length present outside the ring. Moreover, the calculated values of C–H bond lengths of methyl part according to B3LYP and HF methods are also in good agreement.

4.3. Molecular electrostatic potential analysis

Electrostatic potential maps illustrate the charge distributions of molecules three dimensionally. The molecular electrostatic potential (MEP) at point r in space around a molecule (in atomic units) can be expressed as:

$$V(r) = \sum_A \frac{ZA}{\left|\vec{RA} - \vec{r}\right|} - \int \frac{\rho(\vec{r'})\, dr'}{\left|\vec{r'} - \vec{r}\right|} \quad (1)$$

where Z_A is the charge on nucleus A, located at R_A and is the electronic density function for the molecule. The MESP mapped surface of the compounds and electrostatic potential contour map for highest unoccupied molecular orbital (HOMO) and lowest unoccupied molecular orbital (LUMO) potentials are shown in Fig. 2. The scheme-coded values are then projected onto the 0.02 a.u. isodensity surface to produce a three-dimensional electrostatic potential model [17, 18]. Local negative electrostatic potentials (dotted line) signal nitrogen and oxygen atoms with lone pairs whereas local positive electrostatic potentials (continuous line) signal polar hydrogen in C–H bonds.

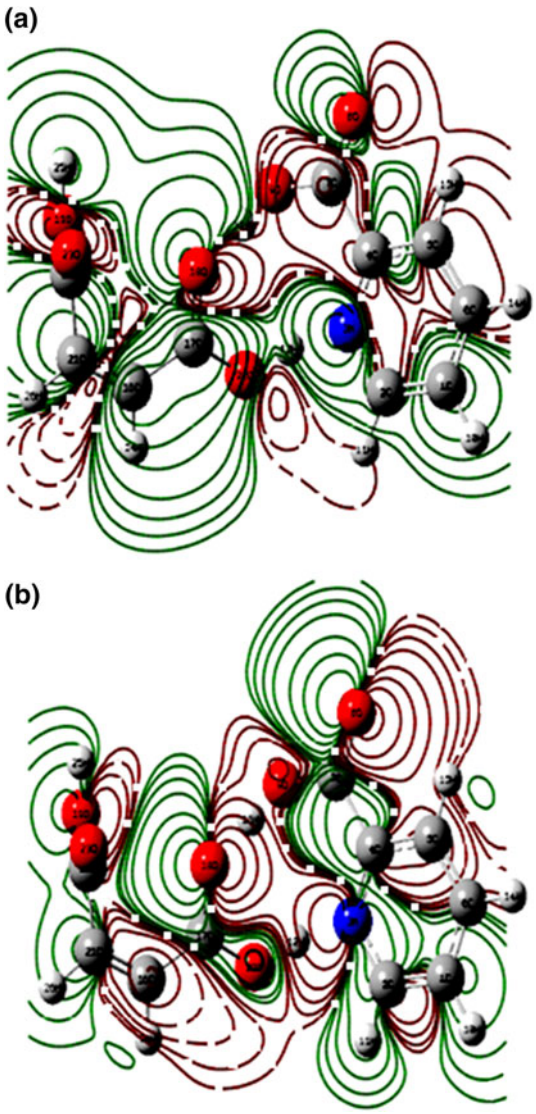

Fig. 2 Electrostatic potential contour map of PM (**a**) HOMO and (**b**) LUMO potentials using 6-311G(d,p) basis set

5. Vibrational analysis

Vibrational spectral assignments have been performed on the recorded FT-IR (powder) spectrum based on the theoretically predicted wavenumbers by ab initio B3LYP. The calculated and scaled vibrational wavenumbers are collected in Table 1 with the scaling factor of 0.96 [19] for B3LYP level. All 72 fundamental modes of vibrations are active. Figure 3 shows the observed spectrum of PM crystal and the simulated spectra of PM molecule at HF/DFT level using 6-311G(d,p) basis sets.

5.1. Carbon–carbon vibrations

In pyridine derivatives, the carbon–carbon stretching modes of vibration appear in the region 1,650–1,200 cm^{-1} and are determined by nature of substituent around the ring [20, 21]. Pyridines and pyrimidines absorb majorly in the region 1,600–1,450 cm^{-1} due to C–C vibrations. This is evidence of presence of bands around 1,500 cm^{-1} in spectrum of the compound [22]. The band observed at 1,472 cm^{-1} in the FTIR spectrum is assigned to CC stretching vibrations. The CC aromatic stretch, known as semicircle stretching predicted at 1,474 cm^{-1} in HF and 1,482 cm^{-1} in DFT are in excellent agreement with experimental observations in FTIR spectrum. The ring deformation at 730 cm^{-1} in HF coincides satisfactorily with the medium band at 650 cm^{-1} and sharp band at 890 cm^{-1} both in FTIR spectrum.

5.2. Hydrocarbon vibrations

C–H stretching vibrations of the pyridine ring are assigned to bands observed at 3,252 cm^{-1} and 3,170 cm^{-1}, also a sharp peak at 3,099 cm^{-1} in IR spectrum of PM. It is noticed that

Table 1 Observed and calculated FTIR frequencies determined by B3LYP method with 6-311G(d,p) basis sets along with their relative intensities, probable assignments of PM

Observed wavenumber FTIR cm^{-1}	HF			DFT			Assignments
	Unscaled	Scaled	Relative intensity	Unscaled	Scaled	Relative intensity	
3,428 (m)	3,666	3,421	86.44	3,462	3,427	20.18	ν(OH) of Maleic acid
	3,439	3,095	7.63	3,259	3,226	6.21	ν(NH) of Picolinic acid
	3,431	3,088	0.53	3,255	3,222	0.74	ν(NH) of Picolinic acid
	3,411	3,070	0.38	3,240	3,208	0.23	ν(OH) of Maleic acid
	3,406	3,065	0.75	3,230	3,198	2.78	ν(OH) of Picolinic acid
3,252 (m)	3,384	3,046	2.71	3,218	3,186	2.81	ν(CH) of Maleic acid
3,120 (m)	3,356	3,020	0.14	3,184	3,152	0.37	ν(CH) of Maleic acid
3,099 (sh)	3,040	2,736	317.69	2,303	2,280	87.17	ν(CH) of Picolinic acid
2,555 (s)	2,734	2,570	263.15	1,892	1,854	66.31	ν(OH) transfer/overtones and combination modes
	1,970	1,852	283.59	1,775	1,740	201.02	ν(C=O) of Maleic acid
2,047 (s)	1,938	1,822	40.88	1,715	1,681	37.71	ν(CO) of Maleic acid
	1,884	1,771	440.61	1,699	1,665	51.60	ν(CC) of Maleic acid
	1,827	1,717	301.06	1,687	1,653	263.19	α(COH) of Maleic acid + α(NHO) of Picolinic acid
1,743 (s)	1,798	1,690	541.70	1,646	1,613	55.66	ν(C=O) of acid group
	1,792	1,684	16.61	1,574	1,543	47.16	α(COH + NHO + CCH)
	1,699	1,597	45.24	1,556	1,525	361.04	ν(ring CC) + α(CCH + CNH)
1,638 (s)	1,635	1,537	156.89	1,508	1,478	103.39	α(ring CCC + CNC + COH)
	1,614	1,517	127.97	1,465	1,436	230.45	λ(COH) + β(COO)
	1,545	1,452	20.78	1,427	1,398	309.20	α(CCH + NHO)
1,595 (ms)	1,541	1,449	24.84	1,421	1,393	180.86	α(NHO + COH + CCH)
	1,492	1,402	100.51	1,378	1,350	35.89	β(COH + CCO + CCH)
1,523 (ms)	1,447	1,360	313.59	1,340	1,313	113.52	β(COH + CCH) + α(CCH)
	1,433	1,347	255.63	1,329	1,302	42.77	α(OHO) + β(CCH)
1,451 (ms)	1,423	1,338	161.28	1,316	1,290	213.25	β(COO + OHO + CCO)
	1,397	1,313	61.10	1,295	1,269	196.19	α(NCH + CCH + CCC + NCC)
1,395 (ms)	1,339	1,259	21.26	1,245	1,220	21.26	α(CCH)
	1,333	1,253	22.05	1,234	1,222	56.18	α(CCH)
1,303 (ms)	1,302	1,224	9.77	1,220	1,208	9.76	ν(C–CO_2) + α(CCH) + δ(ring)
	1,260	1,210	60.27	1,201	1,189	91.63	ν(ring CC) + α(ring CCC)
1,218 (m)	1,237	1,188	3.42	1,174	1,162	86.14	β(CCO + COH)
	1,232	1,183	442.60	1,124	1,113	16.25	δ(ring) + β(NOH + CNH)
1,151 (ms)	1,198	1,150	18.43	1,108	1,097	183.31	β(CCH + COH)
	1,185	1,138	61.38	1,089	1,078	2.65	τ(COH + CCH)
1,085 (s)	1,176	1,129	6.01	1,051	1,040	7.95	β(CCH + NCH)
	1,171	1,124	91.15	1,037	1,027	4.61	β(CCH + NHO)
1,008 (ms)	1,144	1,098	5.36	1,028	1,018	5.44	β(CCO + CCH)
	1,107	1,063	7.24	1,027	1,017	17.09	μ(ring)
936 (sh)	1,092	1,048	0.21	967	957	0.50	τ(COH + NHO)
	1,032	991	20.07	955	945	17.84	β(CCH + NHO)
867 (sh)	948	910	2.71	858	849	13.04	∑(ring)
	945	936	67.81	849	841	43.35	∑(ring)
765 (ms)	910	901	23.91	836	828	19.85	λ(COO) + β(CCO)
	903	894	61.41	823	815	71.56	∑(ring)
	888	879	138.78	811	803	58.78	ν(C–CO_2) + α(CCO)

Table 1 continued

Observed wavenumber FTIR cm^{-1}	HF			DFT			Assignments
	Unscaled	Scaled	Relative intensity	Unscaled	Scaled	Relative intensity	
679 (sh)	850	842	22.16	786	778	5.02	$\nu(C–CO_2) + \alpha(C–OH)$
	818	810	10.73	737	730	24.07	μ(ring) + β(CCC + CCO)
	779	771	13.89	723	716	15.25	τ(ring) + β(NCC + CCC + CCH)
	773	765	79.31	710	703	34.43	$\sum$(ring)
	722	715	85.42	674	667	163.30	τ(ring) + Lattice vibrations
591 (ms)	709	702	46.34	648	642	49.49	ε(ring) + lattice vibrations of Maleic acid
	633	627	164.73	611	605	62.47	β(COH + CCO)
	595	589	21.76	559	553	38.26	β(COH + CCO)
538 (s)	565	559	66.14	530	525	47.68	β(COH + CCO)
	532	527	37.60	500	495	28.01	$\tau(C–CO_2)$
	527	522	0.03	481	476	1.00	ω(CCO + CNH)
	503	498	6.50	455	450	8.34	ω(ring) + β(COH + CCC)
	489	484	0.08	445	441	0.87	ω(picolinic acid)
	402	362	39.15	406	402	51.60	ω(picolinic acid) + lattice vibrations

m medium, *s* small, *sh* sharp, *ms* medium small

ν, stretch; α, in-plane bend; β, out-of-plane bend; λ, scissoring; δ, distorsion; τ, twist; μ, breathing; $\sum$, butterfly; ω, wagging; ε, cradle

C–H stretching mode do not couple with each other. The bands in the range 3,100–3,000 cm^{-1} are due to C–H stretching vibrations in aromatic compounds. The fundamental modes observed at 2,555 cm^{-1} in IR spectra are assigned to C–H stretch with combination and overtones, C–H in plane and out of plane bending vibrations are observed in the region 1,350–950 cm^{-1}. In substituted pyridine derivatives, C–H in plane bending vibration appears in the frequency region 1,550–1,000 cm^{-1} [23, 24]. Normally, the bands are very weak. In our study the bands observed at 1,028, 1,330 cm^{-1} in FTIR spectrum are assigned to C–H in plane bending vibrations and these values are in good agreement with the calculated values. Krishnakumar et al. [25] have been assigned C–H out of plane bending vibrations in the region 986–825 cm^{-1} in FTIR spectrum. The bands observed at 960 in FTIR are assigned to C–H out of plane bending vibrations.

5.3. Nitro-carbon vibrations

Primary aromatic amine with nitrogen directly in the ring absorbs strongly at 1,330–1,260 cm^{-1} due to stretching of the phenyl carbon–nitrogen bond [26]. Silverstein et al. [27] assigned C–N stretching absorption in the region 1,342–1,220 cm^{-1}. The spectra of benzene and pyridyl substituted compounds show bands in the region of 1,260–1,210 cm^{-1}. In analogy with previous work, the band appears at 1,226 cm^{-1} and band at 1,284 cm^{-1} in FTIR spectrum of PM is assigned to C–N symmetric and asymmetric stretching mode of vibrations, respectively. The FTIR spectrum shows complicated pattern of absorption in the region of 3,400–2,700 cm^{-1} originated from N–H stretching mode involved in N–H···O bonds between picolinic acid and mealic acid. The band observed at 1,310 cm^{-1} in infrared is assigned to C–N stretching mode vibrations coupled with the in-plane pyridine ring deformation. The band at 1,425 cm^{-1} is assigned to C–N stretching with some contribution from N–H···O stretch. Medium to weak intensity bands in the frequency range 600–400 cm^{-1} are due to C–N–C deformation vibrations. The peaks at 570, 540, 480, and 420 cm^{-1} are assigned for C–N–C deformation [28]. The assignments of C–N in-plane and out-of-plane bending vibrations made in this study are also supported by literature [29].

5.4. Carbonyl vibrations

The interaction of carbonyl group with the hydrogen donor group does not produce such drastic change in the frequency C=O stretch, as done by interaction of NH stretch. The carbonyl group of maleic acid may interact with other atoms in the molecule and gives rise to a complex pattern of spectrum. As the intermolecular hydrogen bond in maleic acid is very strong, it forms crystalline maleate of various organic molecules through hydrogen bonding and π–π interactions, but acts as a acceptor [30]. The band due to C=O stretching vibration is observed in the region 1,850–1,550 cm^{-1} due to tautomerism, pyrimidines

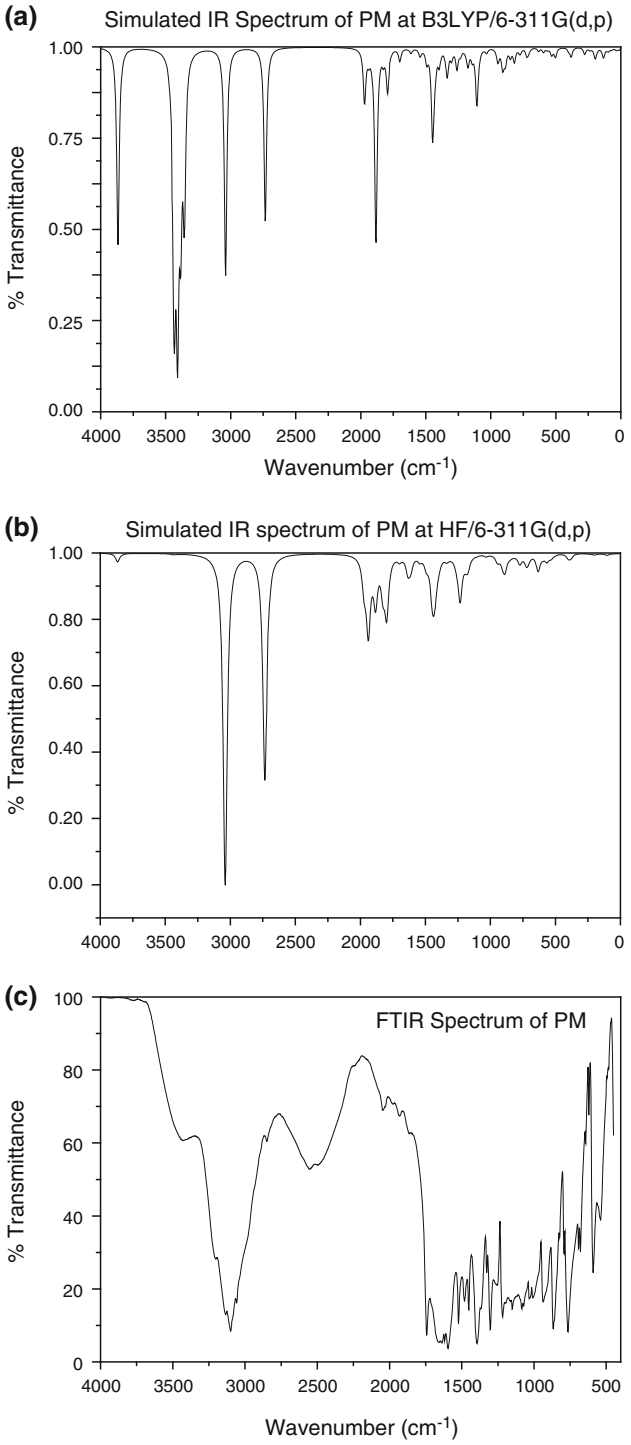

Fig. 3 Simulated spectrum at (**a**) DFT/6-311G(d,p), (**b**) HF/6-311G(d,p) basis sets and (**c**) FTIR spectrum of Picolinium maleate molecule

substituted with hydroxyl groups are generally in the keto form and therefore have a strong band due to carbonyl group [31]. In the present work, a sharp band at 1,743 in FTIR spectrum is assigned to C=O stretching vibrations. In general, the characteristic C=O stretching vibrations of cyclic ketones are found over a relatively wide range depending on the ring size.

5.5. Bending vibrations

The strong band in FTIR at 1,446 cm^{-1} is assigned to N–HO stretching while the bands below 400 cm^{-1} in the calculated spectra are assigned to N–HO in and out of plane bending vibrations. Normally, the deformation modes of C–N–H occur in the region 1,450–1,320 cm^{-1}. Hence, in the present work, the bands appear at 1,330 and 1,420 cm^{-1} in FTIR spectrum are assigned to C–N–H bending modes of vibrations. The vibrational spectra of substituted phenols and its derivatives N–C–H bending modes are observed in the region 1,500–1,425 cm^{-1}. The band appears at 1,450 cm^{-1} in the FTIR spectrum of PM is assigned to N–C–H bending mode of vibration. C–H deformation frequencies in benzene and its derivatives are found to occur in the region 1,200–1,050 cm^{-1}. In the present study the bands observed at 1,090 and 1,210 cm^{-1} in FTIR of PM are assigned to C–C–H deformation. The C–C–C bending mode always occurs below 600–480 cm^{-1} in isopropyl benzenes. In the present work, the band observed at 540 cm^{-1} and the band at 575 cm^{-1} are assigned to C–C–C bending modes of vibration.

5.6. Scale factor

Comparison of frequencies calculated at HF/6-311G(d,p) and B3LYP/6-311G(d,p) basis sets with experimental values reveals that theoretical values give reasonable deviations from the experimental values (see Table 1). To determine the scale factors, the procedure used previously [32] has been followed, that minimizes residual separating experimental and theoretically predicted vibrational frequencies. The optimum scale factors for vibrational frequencies have been determined by minimizing the residual

$$\Delta = \sum_{i}^{N} \left(\lambda_{\omega_i}^{T} - \nu_i^{E} \right)^2 \tag{2}$$

where λ_{wi}^{T}, ith theoretical harmonic frequency and ν_i^{E}, ith experimental fundamental frequency (in cm^{-1}), respectively, and N is the number of frequencies included in the optimization which leads to

$$RMS = \sqrt{\frac{\Delta}{N}} \tag{3}$$

The scale factors used in this study minimized the deviations between the computed and experimental frequencies.

Table 2 The electric dipole moment μ(D), the average polarizability α_{tot} ($\times 10^{-24}$ esu) and first hyperpolarizability β_{tot} ($\times 10^{-30}$ esu) of PM by B3LYP/6-311G(d, p) and HF/6-311G(d,p)

B3LYP/6-311G(d,p)				HF/6-311G(d,p)			
α Components		β Components		α Components		β Components	
μ_x	5.2019	β_{xxx}	99.5546	μ_x	−5.6204	β_{xxx}	−145.0183
μ_y	−6.8364	β_{xxy}	−46.4620	μ_y	−8.5857	β_{xxy}	−76.0248
μ_z	−0.0755	β_{xyy}	−40.0482	μ_z	1.5167	β_{xyy}	44.7575
$\mu_{(D)}$	−8.5908	β_{yyy}	42.8566	$\mu_{(D)}$	10.3732	β_{yyy}	−57.3739
α_{xx}	−65.4542	β_{xxz}	−15.3956	α_{xx}	−66.1775	β_{xxz}	44.4401
α_{xy}	−10.5701	β_{xyz}	15.5492	α_{xy}	9.6609	β_{xyz}	22.0574
α_{yy}	−96.8997	β_{yyz}	−4.8021	α_{yy}	−101.3477	β_{yyz}	10.5021
α_{xz}	8.6734	β_{xzz}	6.2491	α_{xz}	6.4483	β_{xzz}	3.4132
α_{yz}	−3.0409	β_{yzz}	7.2848	α_{yz}	5.1410	β_{yzz}	12.0156
α_{zz}	−102.2866	β_{zzz}	−7.4689	α_{zz}	−101.5698	β_{zzz}	0.6741
α_{tot} (esu)	168.289	β_{tot} (esu)	237.083	α_{tot} (esu)	118.578	β_{tot} (esu)	122.354

6. Molecular polarizability

It is proposed that investigation should be done to see the effect of basis set on molecular polarizability of PM. The first hyperpolarizability is a third-rank tensor that can be described by 10 components in a 3 × 3 × 3 matrix due to Lleinmen symmetry [33–36]. The complete equations for calculating the magnitude of total static dipole moment μ, mean polarizability α_0, anisotropy of polarizability Δα and mean first hyperpolarizibility β_0 using the x, y, z components are given by the following equation

$$E = E_0 - \mu_\alpha F_\alpha - \alpha_{\alpha\beta} F_\alpha F_\beta^- - \beta_{\alpha\beta\gamma} F_\alpha \alpha F_\beta F_\gamma + \cdots \quad (4)$$

where E_0 is energy of unperturbed molecules, F_α is field at origin and μ_α, $\mu_{\alpha\beta}$ and $\beta_{\alpha\beta\gamma}$ are components of dipole moment polarizability and first hyperpolarizability, respectively.

The total static dipole moment μ, mean polarizability α_0, anisotropy of polarizability Δα and mean first hyperpolarizability β_0, using the x, y, z components are defined as

$$\mu = \left(\mu_x^2 + \mu_x^2 + \mu_x^2\right)^{1/2} \quad (5)$$

$$\alpha_0 = [\alpha_{xx} + \alpha_{yy} + \alpha_{zz}]/2 \quad (6)$$

$$\Delta\alpha = 2^{-1/2}[(\alpha_{xx} - \alpha_{yy})^2 + (\alpha_{yy} - \alpha_{zz})^2 + (\alpha_{zz} - \alpha_{xx})^2 + 6\alpha_{xx}^2]^{1/2} \quad (7)$$

$$\beta_0 = \left(\beta_x^2 + \beta_y^2 + \beta_z^2\right)^{1/2} \quad (8)$$

$$\beta_x = \beta_{xxx} + \beta_{xyy} + \beta_{xzz} \quad (9)$$

$$\beta_y = \beta_{yyy} + \beta_{xxz} + \beta_{yyz} \quad (10)$$

$$\beta_z = \beta_{zzz} + \beta_{xxz} + \beta_{yyz} \quad (11)$$

Table 3 Theoretical and experimental spectral characteristics of PM

Experimental		Theoretical		
λ (nm)	Abs	λ (nm)	f	Composition
327 (sh)	16.27	297	0.0412	(H − 2 → L + 1) (H → L − 1)
–	–	405	0.016	(L → H + 1)

the DFT calculated first hyperpolarizability of PM is 237.082 esu and dipole moment is −8.590 in Debye are shown in Table 2. The calculated first hyperpolarizability of PM is much higher than that of urea, and the material is best suited for NLO applications.

7. UV–vis analysis

Results of ZINDO calculations of electronic transition energies of PM molecule along with band assignments are presented in Table 3 and they have been compared with experimental data of PM in solvent as shown in Fig. 4. The wavelength belonging to HOMO–LUMO transition and thus maximum wavelength is at 296 nm. The present experiment shows one intense band at 297 nm (sh), and a weak band is observed at 405 nm, respectively. In ZINDO, we have found that it has a sharp band at 346 nm with the configuration of 0.041 (H − 2 → L + 1) and 0.016 (H → L + 1) excited state respectively [37].

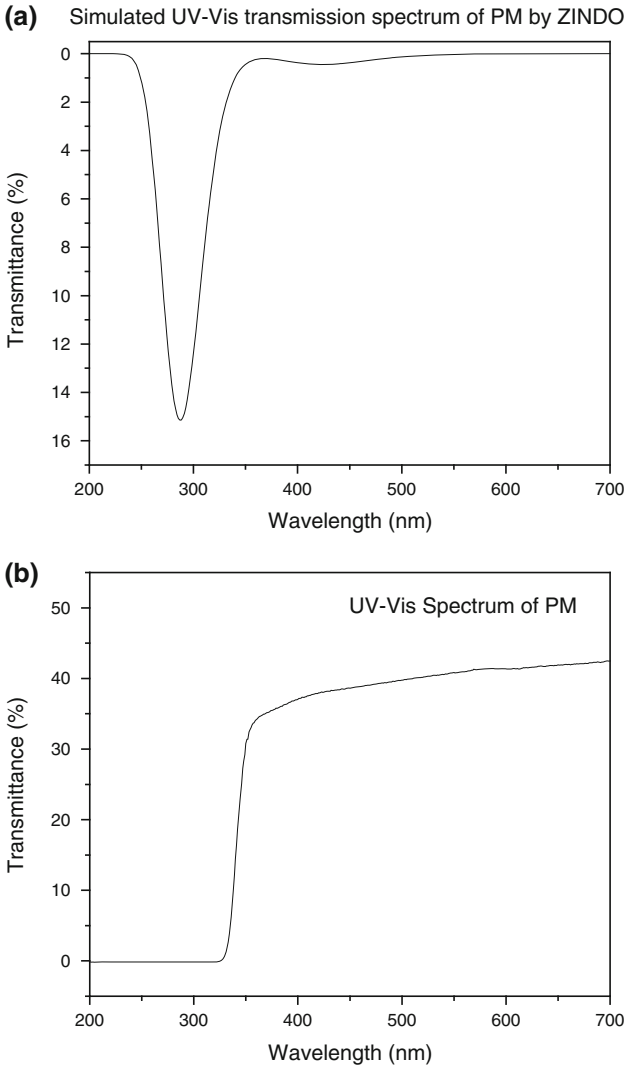

Fig. 4 (**a**) Simulated spectrum using ZINDO basis set and (**b**) UV spectrum of Picolinium maleate crystal

7.1. HOMO, LUMO energy gap

Both HOMO and LUMO are the main orbitals which take part in chemical stability

HOMO energy = −8.9697 eV
LUMO energy = −1.5477 eV
HOMO–LUMO energy gap = −10.5174 eV

The HOMO and LUMO energy gap explains the eventual charge transfer interactions taking place within the molecule.

7.2. Ionization potential

The ionization potential and chemical hardness of the molecule have been calculated using Koopman's theorem [38] and are given by

Table 4 Gross atomic charges of PM

Atom with numbering	HF/6-311G(d,p)	B3LYP/6-311G(d,p)	1H and 13C NMR chemical shift (δ)/ppm
C1	−0.031468	−0.066567	130.2
C2	−0.05413	0.056499	141.1
N3	−0.00606	−0.276937	
C4	0.47557	0.10152	142.4
C5	−0.627443	−0.06394	131.9
C6	0.075784	−0.030664	148.1
C7	0.075392	0.28195	168
O8	0.290432	−0.251787	
O9	−0.490819	−0.36905	
H10	−0.303627	0.087761	6.63
H11	0.055654	0.093234	9.65
H12	−0.507336	0.298909	11.2
H13	0.242145	0.103257	6.78
H14	−0.031468	0.088941	6.66
H15	−0.05413	0.265092	11.1
C16	−0.00606	−0.077795	128.7
C17	0.47557	0.295284	162.5
O18	−0.627443	−0.319226	
O19	0.075784	−0.285138	
C20	0.075392	0.32089	170.6
C21	0.290432	−0.039352	139
O22	0.490819	−0.347549	
O23	−0.303627	−0.256873	
H24	0.055654	0.087171	6.79
H25	−0.507336	0.210754	6.63
H26	0.242145	0.093619	9.96

$$\eta = \frac{(IP - EA)}{2} \tag{12}$$

where $IP \approx -E(HOMO)$, $EA \approx -E(LUMO)$; IP = ionization potential (eV), EA = electron affinity (eV).

The ionization potential has been calculated for PM (5.258 eV) and the effect of substitution of maleic acid in picolinic acid decreases the ionization potential of picolinic acid. One can also relate the stability of the molecule to hardness, which means that the molecule with least HOMO–LUMO gap is more reactive.

8. NMR analysis

The gauge including atomic orbital (GIAO) method is used in calculations of NMR shielding constants. The shielding constants are frequently converted to NMR chemical shifts by calculating a reference compound, which is picolinic acid. The gross atomic charges of PM are given in Table 4.

This data would be useful in identifying the preferred position of the molecule for nucleophilic attack due to charge transfer between molecules [39]. The carbon attached to N and O has lesser electron density than other carbons and hence these are more unshielded. From calculated values, atoms C7 and C17 have nucleophilic centers that share charge transfer during crystallization by hydrogen bonding. Further, the bond distance between C–O···H is 1.428 A confirming nucleophilic attraction between maleic acid and picolinic acid. Hence, we compare the gross atomic charges of PM with calculated 1H and 13C NMR chemical shifts.

9. Conclusions

Attempts have been made in the present work to obtain the proper frequency assignments for the crystal PM from FT-IR and UV–vis spectra. The equilibrium geometries, harmonic frequencies and IR spectra of PM have been determined and analyzed both at HF and DFT levels of theory utilizing 6-311G(d,p) basis set, giving allowance to the lone pairs through diffuse functions. Comparison between calculated vibrational frequencies and experimental values indicates that both the methods of B3LYP/6-311G(d,p) and HF/6-311G(d,p) can predict IR and UV spectra of the title compound well. Any discrepancy noted between observed and calculated frequencies may be due to the fact that calculations have been actually done on a single molecule in gaseous state contrary to experimental values recorded in the presence of intermolecular interactions.

Acknowledgments The authors are thankful to Prof. Dr. R. Mohan Kumar, Department of Physics, Presidency College, Chennai, Tamil Nadu, India-600005, for supplying the XRD data and FTIR, UV details used in this study. The authors are also thankful to Prof. E. M. Subramanian, Department of Chemistry, Pachaiyappas College for Men, Kanchipuram, Tamil Nadu, India-631503, for valuable discussion.

References

[1] X Q Wang et al. *J. Crystal Growth* **234** 469 (2002)
[2] X L Duan et al. *Cryst. Res. Technol.* **37** 1066 (2002)
[3] M H Jiang and Q Fang *Adv Mater* **11** 1147 (1999)
[4] J B Gaudry et al. *Chem. Phys. Lett.* **324** 321 (2000)
[5] T Rasheed and S Ahmad *Indian J. Phys.* **85** 239 (2011)
[6] D S Chemla and J Zyss *Nonlinear Optical Properties of Organic Materials and Crystals* (New York: Academic Press) (1987)
[7] S R Marder, J W Perry and W P Schaefer *Science* **245** 626 (1989)
[8] P M Anbarasan, P S Kumar, K Vasudevan, R Govindan and V Aroulmoji *Indian J. Phys.* **85** 1477 (2011)
[9] D Eimerl, S Velsko, L Davis, F Wang, G Loiacona and G Kennedy *IEEE Quantum Electron.* **25** 179 (1989)
[10] G R Kumar, S G Raj, R Mohan and R Jayavel *J. Crystal Growth* **275** 1947 (2005)
[11] C H S Lin, N Gabas, J P Canselier and G Pope *J. Crystal Growth* **191** 791 (1998)
[12] A Deepthy and H L Bhat *J. Crystal Growth* **226** 287 (2001)
[13] S Gunasekaran, G Anand, R A Balaji, J Dhanalakshmi and S Kumaresan *Pramana – J. Phys.* **75** 683 (2010)
[14] M J Frisch et al. Gaussian Inc (Wallingford: CTPA) (2001)
[15] P Pandi et al. *Spectrochim. Acta A* **98** 7 (2012)
[16] A U Rani, N Sundaraganesan, M Kurt, M Cinar and M Karabacak *Spectrochim. Acta* A **75** 1523 (2010)
[17] R H Petrucci, W S Harwood, F G Herring and J D Madura *General Chemistry: Principles & Modern Applications*, 9th edn. (New Jersey: Pearson Education Inc) (2007)
[18] I G Csizmadia *Theory Practice of MO Calculations on Organic Molecules* (Amsterdam: Elsevier) (1976)
[19] J A Pople et al. *Int J. Quantum Chem. Quantum Chem. Symp.* **15** 269 (1981)
[20] L J Bellamy *The Infrared Spectra of Complex Molecules*, 3rd edn. (New York: Wiley) (1975)
[21] G Varsanyi *Assignments for Vibrational Spectra of Seven Hundred Benzene Derivatives* (London: Adam Hilger) (1974)
[22] S Gunasekaran, S R Varadhan and K Manoharan *Asian J. Phys.* **4** 12 (1993)
[23] G Socrates *Infrared and Raman Characteristic Group Frequencies*, 3rd edn. (Chichester: John Wiley & Sons Ltd) (2001)
[24] A P Upadhya and K N Upadhyay *Indian J. Pure Appl. Phys.* **20** 672 (1982)
[25] V Krishnakumar, N Surumbarkuzhali and S Muthunatesan *Spectrochim. Acta A* **71** 1810 (2009)
[26] R Saxena, L D Kauedpal and G N Mathur *J. Polym. Sci. A: Polym Chem* **40** 3559 (2002)
[27] R M Silverstein, G Clayton Basslor and T C Morill *Spectrometric Identification of Organic Compounds* (New York: John Wiley) (1981)
[28] G Socrates *Infrared characteristics group frequencies*, Ed. (Meerut: Pragati Prakashan) (1992)
[29] S Mohan, N Sundaraganesan and J Mink *Spectrochim. Acta A* **47** 1111 (1991)
[30] P Pandi, G Peramaiyan, M Krishna Kumar, R Mohan Kumar and R Jayavel *Spectrochim. Acta Part A* **88** 77 (2012)
[31] S Kumar, A K Rai, S B Rai and D K Rai *Indian J. Phys.* **84** 563 (2010)
[32] V Arujunan, I Saravanan, Mariusz K Marchewka and S Mohan *Spectrochim. Acta Part A* **92** 305 (2012)
[33] M Tommasini, C Castiglioni, M Del Zoppo and G Zerbi *J. Mol. Structure* **480** 179 (1999)
[34] C R Zhang, H S Chem and G H Wang *Chem. Res. Chin. Univ.* **20** 640 (2004)
[35] P S Kumar, K Vasudevan, A Prakasam, M Geetha and P M Anbarasan *Spectrochim. Acta A* **77** 45 (2010)
[36] D A Kleinman *Phys. Rev.* **126** 1977 (1962)
[37] S Gunasekaran, S Kumaresan, R Arunbalaji, G Anand, S Seshadri and S Muthu *J. Raman Spectroscopy* **40** 1675 (2009)
[38] T A Koopmans *Physica* **1** 104 (1933)
[39] S Gunasekaran, R A Balaji, S Kumaresan, G Anand and S Srinivasan *Canadian J. Anal. Sci.Spectr.* **53** 149 (2008)